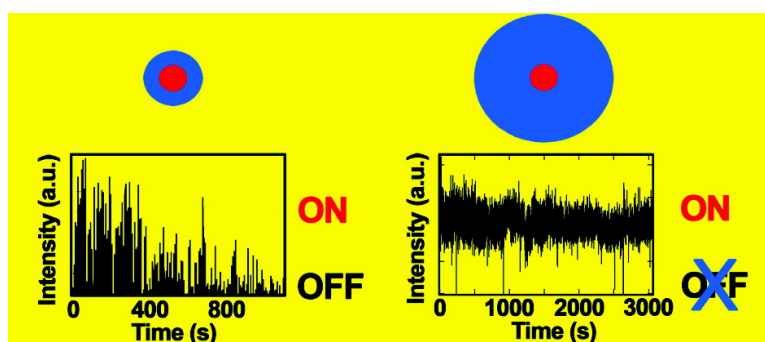


## “Giant” Multishell CdSe Nanocrystal Quantum Dots with Suppressed Blinking

Yongfen Chen, Javier Vela, Han Htoon, Joanna L. Casson, Donald J. Werder, David A. Bussian, Victor I. Klimov, and Jennifer A. Hollingsworth

*J. Am. Chem. Soc.*, **2008**, 130 (15), 5026-5027 • DOI: 10.1021/ja711379k • Publication Date (Web): 20 March 2008

Downloaded from <http://pubs.acs.org> on February 8, 2009



### More About This Article

Additional resources and features associated with this article are available within the HTML version:

- Supporting Information
- Links to the 8 articles that cite this article, as of the time of this article download
- Access to high resolution figures
- Links to articles and content related to this article
- Copyright permission to reproduce figures and/or text from this article

[View the Full Text HTML](#)

## “Giant” Multishell CdSe Nanocrystal Quantum Dots with Suppressed Blinking

Yongfen Chen, Javier Vela, Han Htoon, Joanna L. Casson, Donald J. Werder, David A. Bussian, Victor I. Klimov, and Jennifer A. Hollingsworth\*  
Chemistry Division, Los Alamos National Laboratory, Los Alamos, New Mexico 87545

Received December 23, 2007; E-mail: jenn@lanl.gov

Semiconductor nanocrystal quantum dots (NQDs) are considered near-ideal fluorophores based on their unique particle-size-tunable optical properties—efficient broadband absorption and narrow-band emission. Further, compared to alternative fluorophores, such as organic dyes, NQDs are characterized by significantly enhanced photostability.<sup>1</sup> Despite these enabling characteristics, NQD optical properties are frustratingly sensitive to their surface chemistry and chemical environment. The coordinating organic ligands used to passivate the NQD surface during growth are retained following preparation and are strong contributors to such bulk NQD optical properties as quantum yields (QYs) in emission. Unfortunately, ligands are labile and can become uncoordinated from the NQD surface, and as organic molecules, they can be damaged by exposure to the light sources used for NQD photoexcitation. Ligand loss through physical separation or photochemistry results in uncontrolled changes in QYs and, in the case of irreversible and complete loss, in permanent “darkening” or photobleaching.

In addition, NQDs are characterized by significant “blinking” (fluorescence intermittency) at the single NQD level.<sup>2</sup> While a precise mechanism has yet to be universally accepted, blinking is generally considered to arise from an NQD charging process in which an electron (or a hole) is temporarily lost to the surrounding matrix (Auger ejection or charge tunneling) or captured to surface-related trap states.<sup>2–4</sup> NQD emission turns “off” when the NQD is charged and turns “on” again when NQD charge neutrality is regained. Blinking is unacceptable for such potential NQD applications as single-photon light sources for quantum informatics and biolabels for real-time monitoring of single biomolecules.

Here, we report for the first time that these key optical properties—QY, photobleaching, and blinking—can be rendered independent of NQD surface chemistry and chemical environment by growth of a very thick inorganic shell. It is known that addition of an inorganic shell of a higher bandgap semiconductor material (e.g., ZnS onto CdSe) can generally enhance QYs and improve stability.<sup>5–7</sup> However, the optical properties of standard core/shell and core/multishell NQDs remain susceptible to ligand loss, changes in ligand identity through ligand-exchange reactions, and/or ligand concentration.<sup>8,9</sup> Further, others have previously reported the use of so-called “antiblinking reagents”<sup>10</sup> to suppress blinking.<sup>11–13</sup> Such reagents likely serve as charge mediators or charge compensators.<sup>8,10,12,13</sup> In contrast, our approach is to fully isolate the wave function of the NQD core from the NQD surface and surface environment. In this way, we create a fundamentally unique NQD that is structurally more akin to physically grown epitaxial QDs, for which optical properties are stable and blinking is not observed.<sup>14</sup>

Starting with 3–4 nm NQD CdSe cores (Figure 1a), we grew the particles to a size of 15–20 nm (Figure 1b,c) by sequentially applying monolayers of inorganic shells. The shell layers of CdS, ZnS, or Cd<sub>x</sub>Zn<sub>1-x</sub>S alloys were grown onto CdSe cores using

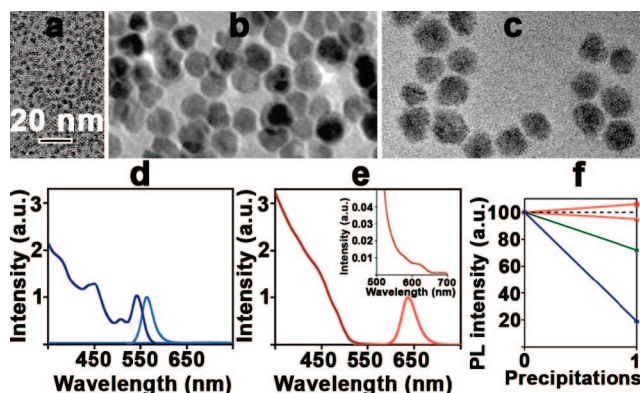


**Figure 1.** Transmission electron microscopy (TEM) images for (a) CdSe NQD cores, (b) CdSe/19CdS g-NQDs, and (c) CdSe/11CdS-6Cd<sub>x</sub>Zn<sub>1-x</sub>S-2ZnS g-NQDs. (d) Absorption (dark blue) and PL (light blue) spectra for CdSe NQD cores. (e) Absorption (dark red) and PL (light red) spectra for CdSe/19CdS g-NQDs (inset: absorption spectrum expanded to show contribution from core). (f) Normalized PL compared for growth solution and first precipitation/redissolution for CdSe/11CdS-6Cd<sub>x</sub>Zn<sub>1-x</sub>S-2ZnS and CdSe/19CdS g-NQDs (red), CdSe/2CdS-2ZnS and CdSe/2CdS-3Cd<sub>x</sub>Zn<sub>1-x</sub>S-2ZnS NQDs (green), and CdSe core NQDs (blue). Dashed line indicates no change.

modified literature procedures based on a successive ion layer absorption and reaction (SILAR) method.<sup>9,15</sup> The growth of nominally 18–19 monolayers of shell material (calculated based on the amount of shell precursor added) was conducted over a period of 5 days with reasonable control over size dispersity (Figure 1b,c) and retention of a regular, faceted particle shape (see Supporting Information Figure S-1). The shell is either single-component—CdSe/19CdS NQDs (Figure 1b; 15.5 ± 3.1 nm)—or multicomponent—CdSe/11CdS-6Cd<sub>x</sub>Zn<sub>1-x</sub>S-2ZnS (Figure 1c; 18.3 ± 2.9 nm), where the six layers of alloyed shell material (6Cd<sub>x</sub>Zn<sub>1-x</sub>S) are successively richer in Zn (from nominally 0.13 to 0.80 atomic % Zn).

These “giant” NQDs (g-NQDs) are characterized by photoluminescence (PL) spectra that are shifted to longer wavelengths (lower energies) compared to the original NQD cores (for example, Figure 1e; PL maximum is 638 nm), and no emission from the shell is observed. Such extensive “red shifting” is also known for standard multishell NQDs<sup>9</sup> and indicates extension of the NQD core wave function into the shell region, which increases the effective size of the core and reduces the quantum confinement felt by the semiconductor wave function. In contrast to PL, g-NQD absorption spectra are dominated by the shell material. This is not unexpected as, at these sizes, the shell:core volume ratio is approximately 100:1. In the example shown here (Figure 1e), the shell is made up of nominally 19 monolayers of CdS, and the principal absorption onset of this g-NQD is at ~500 nm, reflective of the CdS bulk bandgap. However, a separate absorption feature

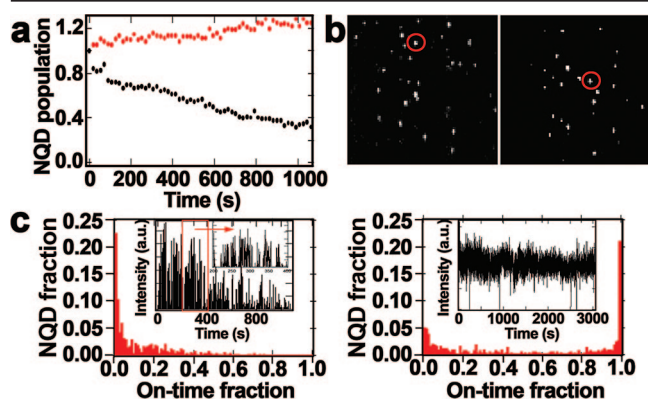


**Figure 2.** Single NQD studies. (a) Emitting NQD fraction over time: Qdot655ITK (black); g-NQD CdSe/19CdS (red). (b) Fluorescence image and (c) on-time histograms of Qdot655ITK (left) and CdSe/19CdS g-NQD (right). Insets in (c) show fluorescence time traces of the circled NQDs in (b). Temporal resolution is 200 ms.

is also present and represents the absorption onset of the core CdSe (spatially extended as described above by the presence of the shell material). This feature occurs clearly at  $\sim 620$  nm (Figure 1e, inset) and exhibits spectral fine structure that is indicative of a good size dispersion. Thus, the PL and absorption data demonstrate that, despite the enormously long reaction times, the integrity of the optically active core is not compromised.

g-NQDs are uniquely insensitive to changes in ligand concentration and identity, and the chemical stability afforded by the g-NQDs clearly surpasses that of the standard multishell and core-only NQDs. Specifically, we observed that, upon precipitation from growth solution and redissolution in hexane, the QYs for g-NQDs did not change ( $\pm 5\%$ ; Figure 1f). In contrast, QYs for standard multishell NQDs, such as CdSe/2CdS-2ZnS and CdSe/2CdS-3Cd<sub>2</sub>Zn<sub>3</sub>S-2ZnS (where  $x$  is varied successively from 0.13 to 0.80), dropped by approximately 30% (Figure 1f), while those for core-only samples dropped by more than 80% (Figure 1f). Further, we precipitated and redissolved g-NQDs seven times and observed no changes in QY, nor did we observe any change in QY upon transfer to water using a standard ligand exchange procedure (replacing as-prepared ligands with mercaptosuccinic acid).

The absolute QYs for g-NQDs have yet to be optimized, however. While QYs for the all-CdS version described above were high, approximately 40%, those for the alloy g-NQDs and a CdSe/10CdS-8ZnS version were only 10%. In contrast, we typically obtained QYs for the standard, thinner multishell NQDs of 80–90%. Reduced QY in traditional NQDs is typically explained by incomplete surface passivation by ligands. In the case of g-NQDs, the mechanism is likely different and related, instead, to recombination through defects (dislocations, etc.) within the thick, imperfect shell.<sup>16</sup>

Perhaps more remarkably still, the g-NQDs are stable under continuous laser illumination (532 nm, 205 mW laser) at a single-dot level. Specifically, freshly diluted g-NQDs in either toluene or water were dispersed onto a clean quartz slide. Samples were irradiated for several hours at a time over several days. Photobleaching was not observed in either the samples deposited from toluene or the samples deposited from water. This result stands in stark contrast with those obtained for control samples. Namely, core-only samples, as well as the thinner multishell samples, photobleached (complete absence of PL) within 1 s, and commercial NQDs (Qdot655ITK) photobleached with a  $t_{1/2} \approx 15$  min (Figure 2a).

Under these continuous excitation conditions, significantly suppressed blinking behavior was observed for all g-NQDs versus control samples (Figure 2b,c). The distinctive single NQD fluorescence behavior and the blinking statistics for a large population ( $>500$ ) of single g-NQDs and Qdot655ITK NQDs is presented in Figure 2c. Typical of classically blinking NQDs,  $>70\%$  of the Qdot655ITK NQDs have on-time fractions (fraction of total observation time that a single NQD is on) of  $<0.2$ . In contrast,  $>20\%$  of the g-NQDs are nonblinking—have an on-time fraction of  $>0.99$ —and  $>40\%$  of these NQDs have an on-time fraction of  $>0.8$ . Dynamic light scattering (DLS) data for the solutions used to make the thin films showed no evidence for clustering or aggregation of the g-NQDs, and their DLS-extracted hydrodynamic diameters (HDs) were consistent with those derived from TEM plus two ligand layers (Supporting Information).

We have shown that, by growing very thick inorganic shells onto CdSe cores, a functionally unique class of NQDs can be realized. In comparison with traditional NQDs, the g-NQDs exhibit unparalleled chemical robustness, photostability with respect to photobleaching, and significantly modified blinking behavior, where a substantial fraction ( $>20\%$ ) of the g-NQDs are nonblinking over long times. These characteristics will enable applications from biology to optoelectronics that were previously hindered by ensemble and single NQD instabilities. The 15–20 nm particle size should not prove limiting for many single-particle tracking applications, where significantly larger probes are frequently used.<sup>17,18</sup> Efforts to confirm the proposed structure–function relationship are ongoing.

**Acknowledgment.** Research supported by LANL LDRD and the DOE Center for Integrated Nanotechnologies (J.A.H. and V.I.K.).

**Supporting Information Available:** High-resolution TEM and experimental details. This material is available free of charge via the Internet at <http://pubs.acs.org>.

## References

- Jaiswal, J. K.; Mattoussi, H.; Mauro, J. M.; Simon, S. M. *Nat. Biotechnol.* **2003**, *21*, 47–51.
- Nirmal, M.; Dabbousi, B. O.; Bawendi, M. G.; Macklin, J. J.; Trautman, J. K.; Harris, T. D.; Brus, L. E. *Nature* **1996**, *383*, 802–804.
- Banin, U.; Bruchez, M.; Alivisatos, A. P.; Ha, T.; Weiss, S.; Chemla, D. S. *J. Chem. Phys.* **1999**, *110*, 1195–1201.
- Kuno, M.; Fromm, D. P.; Hamann, H. F.; Gallagher, A.; Nesbitt, D. J. *J. Chem. Phys.* **2001**, *115*, 1028–1040.
- Hines, M. A.; Guyot-Sionnest, P. *J. Phys. Chem.* **1996**, *100*, 468–471.
- Peng, X.; Schlamp, M. C.; Kadavanich, A. V.; Alivisatos, A. P. *J. Am. Chem. Soc.* **1997**, *119*, 7019–7029.
- Van Sark, W. G. J. H. M.; Frederix, P. L. T. M.; van den Heuvel, D. J.; Gerritsen, H. C.; Bol, A. A.; van Lingen, J. N. J.; de Mello Donega, C.; Meijerink, A. *J. Phys. Chem. B* **2001**, *105*, 8281–8284.
- Jeong, S.; Achermann, M.; Nanda, J.; Ivanov, S.; Klimov, V. I.; Hollingsworth, J. A. *J. Am. Chem. Soc.* **2005**, *127*, 10126–10127.
- Xie, R.; Kolb, U.; Li, J.; Basche, T.; Mews, A. *J. Am. Chem. Soc.* **2005**, *127*, 7480–7488.
- Biebricher, A.; Sauer, M.; Tinnefeld, P. *J. Phys. Chem. B* **2006**, *110*, 5174–5178.
- Hohng, S.; Ha, T. *J. Am. Chem. Soc.* **2004**, *126*, 1324–1325.
- Hammer, N. I.; Early, K. T.; Sill, K.; Odoi, M. Y.; Emrick, T.; Barnes, M. D. *J. Phys. Chem. B* **2006**, *110*, 14167–14171.
- He, H.; Qian, H.; Dong, C.; Wang, K.; Ren, J. *Angew. Chem., Int. Ed.* **2006**, *45*, 7588–7591.
- Pistol, M.-E.; Castrillo, P.; Hessman, D.; Prieto, J. A.; Samuelson, L. *Phys. Rev. B* **1999**, *59*, 10725–10729.
- Li, J. J.; Wang, Y. A.; Guo, W.; Keay, J. C.; Mishima, T. D.; Johnson, M. B.; Peng, X. *J. Am. Chem. Soc.* **2003**, *125*, 12567–12575.
- Dabbousi, B.; Rodriguez-Viejo, J.; Mikulec, F.; Heine, J.; Mattoussi, H.; Ober, R.; Jensen, K.; Bawendi, M. G. *J. Phys. Chem. B* **1997**, *101*, 9463–9475.
- Ritchie, K.; Shan, X.-Y.; Kondo, J.; Iwasawa, K.; Fujiwara, T.; Kusum, A. *Biophys. J.* **2005**, *88*, 2266–2277.
- Saxton, M.; Jacobson, K. *Annu. Rev. Biophys. Biomol. Struct.* **1997**, *26*, 373–399.

JA711379K